Plant Physiol. (1996) 112: 833–844

Targeting of Two Arabidopsis H^+-ATPase Isoforms to the Plasma Membrane[1]

Natalie D. DeWitt, Bimei Hong, Michael R. Sussman, and Jeffrey F. Harper*

Department of Genetics, Yale University School of Medicine, New Haven, Connecticut 06510 (N.D.D.W.); Department of Cell Biology, The Scripps Research Institute, 10550 North Torrey Pines Road, La Jolla, California 92037 (B.H., J.F.H.); and Department of Horticulture, University of Wisconsin, 1575 Linden Drive, Madison, Wisconsin 53706 (M.R.S.)

More than 11 different P-type H^+-ATPases have been identified in Arabidopsis by DNA cloning. The subcellular localization for individual members of this proton pump family has not been previously determined. We show by membrane fractionation and immunocytology that a subfamily of immunologically related P-type H^+-ATPases, including isoforms AHA2 and AHA3, are primarily localized to the plasma membrane. To verify that AHA2 and AHA3 are both targeted to the plasma membrane, we added epitope tags to their C-terminal ends and expressed them in transgenic plants. Both tagged isoforms localized to the plasma membrane, as indicated by aqueous two-phase partitioning and sucrose density gradients. In contrast, a truncated AHA2 (residues 1–193) did not, indicating that the first two transmembrane domains alone are not sufficient for plasma membrane localization. Two epitope tags were evaluated: c-*myc*, a short, 11-amino acid sequence, and β-glucuronidase (GUS), a 68-kD protein. The c-*myc* tag is recommended for its sensitivity and specific immunodetection. GUS worked well as an epitope tag when transgenes were expressed at relatively high levels (e.g. with AHA2-GUS944); however, evidence suggests that GUS activity may be inhibited when a GUS domain is tethered to an H^+-ATPase complex. Nevertheless, the apparent ability to localize a GUS protein to the plasma membrane indicates that a P-type H^+-ATPase can be used as a delivery vehicle to target large, soluble proteins to the plasma membrane.

In fungi and higher plants, protons pumped out of the cell generate a pH gradient and electrical potential across the plasma membrane (Sussman et al., 1994; Michelet and Boutry, 1995). The proton gradient provides the driving force for nutrient uptake through proton-coupled co-transport systems. In addition, the electrical potential plays a role in regulating voltage-gated ion channels. This plasma membrane proton gradient is generated primarily by P-type H^+-ATPases, as demonstrated by biochemical and physiological studies (Briskin, 1990). Thus, P-type H^+-ATPase activity has become accepted as a standard marker for the plasma membrane.

In recent years the identification of plant genes encoding P-type H^+-ATPases has provided new molecular tools for their study. Initially, three genes cloned from Arabidopsis (isoforms AHA1, AHA2, and AHA3) were proposed to encode plasma membrane P-type H^+-ATPases based on protein sequence similarities with (a) the fungal H^+-ATPases and (b) peptide sequences obtained from a 100-kD ATPase protein isolated from oat root plasma membranes (Harper et al., 1989; Pardo and Serrano, 1989). Gene families encoding similar proteins have been found in other plants such as tobacco (Boutry et al., 1989) and tomato (Ewing and Bennett, 1994). The first confirmation that any of these cloned genes encode an ATPase with proton-pumping activity was obtained recently from heterologous expression of isoforms AHA1, AHA2, and AHA3 in yeast (Palmgren and Christensen, 1993, 1994). Nevertheless, to our knowledge, there has not yet been corroboration that any of the cloned genes actually encodes a pump that resides in the plasma membrane.

The 11 different Arabidopsis P-type H^+-ATPase isoforms (Harper et al., 1994; J.F. Harper, unpublished data) make up the largest subfamily of cation-translocating ATPases identified in plants or animals. At least some of these multiple isoforms (e.g. AHA1, AHA2, and AHA3) have distinct kinetic and regulatory properties (Palmgren and Christensen, 1994). This functional diversity raises the possibility that each isoform may be tailored for a particular cellular or subcellular location. Previous investigations established that different isoforms do indeed reside in different tissues and cell types throughout the plant (DeWitt et al., 1991; Ewing and Bennett, 1994; Holné and Boutry, 1994). However, the possibility that some of these isoforms may reside in locations other than the plasma membrane has not previously been investigated.

A precedent for endomembrane-localized P-type H^+-ATPases is provided by immunolocalization studies on the marine alga *Heterosigma akashiwo* (Wada et al., 1994), in which two pumps (most similar to proton pumps identified in higher plants and protozoans) were found to reside in internal membranes. In addition, there is intriguing evidence that some P-type H^+-ATPases may be located in

[1] This research was supported by grants to J.F.H. from the U.S. Department of Agriculture (no. 92–37304–7889) and the Department of Energy (no. DE–FG03–94ER20152) and to M.R.S. from the Department of Energy (no. DE–F602–88ER13938) and from the Department of Energy/National Science Foundation/U.S. Department of Agriculture Collaborative Program in Plant Biology (no. BIR 92–20331).

* Corresponding author; e-mail harper@scripps.edu; fax 1–619–784–9840.

Abbreviation: AHA, Arabidopsis H^+-ATPase.

secretory vesicles that are poised to fuse with the plasma membrane in response to auxin (Hager et al., 1991).

Here we present two complementary approaches for investigating the subcellular localization of the P-type H^+-ATPase multigene family in Arabidopsis. First, we used a polyclonal antiserum to show that the plasma membrane is the primary location for a major subfamily of proton pumps, including isoforms AHA2 and AHA3. However, since our antiserum recognized multiple isoforms, this approach could not be used to determine the localization of a specific isoform. Therefore, we also used an isoform-specific approach, in which isoforms AHA2 and AHA3 were epitope tagged and expressed in transgenic plants and their subcellular location was determined by membrane fractionation. Together, our results indicate that both AHA2 and AHA3 are preferentially localized to the plasma membrane.

MATERIALS AND METHODS

All plant studies were done with *Arabidopsis thaliana* cv Bensheim. DNA cloning was done in *Escherichia coli* strain XL1-Blue (Statagene) or DH10α (BRL). Unless noted, standard molecular techniques were performed according to Sambrook et al. (1989).

Antibodies

Anti-CTF2 rabbit polyclonal antiserum was produced by Promega, using our fusion protein (CTF2), which contained the C-terminal end of AHA2 fused to glutathione *S*-transferase. CTF2 fusion protein was purified from an *E. coli* expression system by affinity purification over a glutathione agarose column (Smith and Johnson, 1988). For immunogold labeling, the antibody was further purified by clearing against glutathione *S*-transferase. Commercially available antibodies used were: mouse anti-c-*myc* monoclonal 9E10.2 (IgG_1) (Oncogene Science, Manhasset, NY); rabbit anti-GUS affinity-purified polyclonal (Clontech, Palo Alto, CA; Molecular Probes, Eugene, OR); rabbit anti-mouse IgG (Cappell, Durham, NC); goat anti-rabbit IgG horseradish peroxidase-conjugated secondary antibody (Amersham); rabbit anti-mouse IgG horseradish peroxidase-conjugated secondary antibody (Cappell); and anti-rabbit IgG alkaline phosphatase-conjugated secondary antibody (Promega).

DNA Constructs

AHA2 C-Terminal End Fusion

pCTF2 encodes a fusion protein with the last 98 residues of AHA2 fused to the carboxyl end of glutathione *S*-transferase. The construct was made by amplifying the DNA sequence encoding the C-terminal end of AHA2 by 12 cycles of a standard PCR (Perkin Elmer). The template used was an AHA2 cDNA previously cloned in the vector pBlueScript SK(−) (Harper et al., 1990). The 5′ side amplification primer contained a *Bam*HI linker (with a reading frame of GGA/TCC) that amplified AHA2-coding sequence downstream of L_{851}. The 3′ side primer was T7. The amplified product contained the entire 3′ untranslated sequence of AHA2 and was inserted into the *Bam*HI/*Eco*RI site in the expression vector pGEX-2T (Smith and Johnson, 1988).

Epitope Cassettes

A GUS cassette of approximately 1.8 kb (GUS-A) was generated with 5′ and 3′ flanking *Bam*HI sites by 12 cycles of a PCR. The template used was pBI-101 (Clontech). The amplification primers GUS3′ and GUS5′ were synthesized with *Bam*HI linkers, providing a reading frame of G/GAT/CC at both 5′ and 3′ ends. Products were cut and cloned into the *Bam*HI site of pBlueScript KS(+) (Stratagene).

A c-*myc* epitope (Kolodziej and Young, 1991) cassette was generated by annealing two partially overlapping complementary oligomers (c-*myc* 2, sense, dAAG GAT CCT CCG GAG CAA AAG CTT ATC AGT GAG; c-*myc* 3, antisense, dG AAG ATC TAG CAA GTC TTC CTC ACT GAT A), making double-stranded DNA strands with Klenow and deoxyribonucleotide triphosphates, and cutting with *Bam*HI and *Bgl*II (sites are underlined).

Epitope-Tagged AHA2 and AHA3

Diagrams for the constructs pAHA2-GUS944, pAHA3-GUS904, and pAHA3-c-*myc*904 are shown in Figure 5. All of the tagged constructs were made with the vector pBIN19, which confers kanamycin resistance to bacterial hosts as well as to transgenic plants (Bevan, 1984). The genomic sequence used for AHA2 constructs was obtained from clone pgAHA2-EES (Harper et al., 1990). The genomic sequence used for AHA3 constructs was obtained from pgAHA3-S and pgAHA3-3′SX (DeWitt and Sussman, 1995). To insert the epitope cassettes at positions corresponding to amino acids 904 and 944, *Bam*HI sites were introduced by site-specific mutagenesis (Kunkel et al., 1987). The mutagenesis primers 2BM-904 dATCTCAG-GATCCTCTCTGTAAC(C/T)(A/T)CCT and 2BM-944 dGT-GGGGATCCG(C/G)(T/A)GT(T/C/A)TCAATGTC created a *Bam*HI site (underlined) with a reading frame of G/GAT/CC in the coding strand (primers shown correspond to the antisense strand). Positions in parentheses were made degenerate.

AHA2-GUS944 was made by the insertion of a GUS-A cassette into the engineered *Bam*HI site and then subcloning the tagged gene into the *Sal*I/*Sac*I site of pBIN19. AHA3-GUS904, AHA3-944, AHA3-c-*myc*904 and AHA3-c-myc-944 were made by the insertion of GUS-A and c-*myc* cassettes into the engineered *Bam*HI site. The tagged AHA3 genes were then subcloned into the *Xba*I/*Sal*I site of the vector pBIN19. The subcloning of AHA3 required multiple steps and resulted in the destruction of the vector's *Xba*I site. However, it should be possible to subclone each tagged construct as a single *Kpn*I/*Sal*I fragment. Each of the tagged constructs was sequenced to confirm the correct in-frame fusion of the epitope cassettes. The sequence at the 944-tagging position of AHA3 was found to have an unplanned mutation resulting in a two-base deletion from the T948 codon (ACC). The altered C-terminal end had the

sequence dCAC CGT TTA ATA AAT ATT **TAA**, where CGT represents the mutated codon, and the new reading frame ending in a TAA stop codon is denoted by spacing. The final sequence of other constructs in the 944 and 904 regions are shown in Figure 6.

Truncated AHA2-GUS Fusion

AHA2-GUS193 was constructed by cloning the *SalI/SmaI* fragment from pgAHA2-EES into the *SalI/SmaI* site of pBI-101.2 (ClonTech) creating an in-frame fusion with the vector's GUS gene. This AHA2 truncation contains the same promoter and upstream sequences as AHA2-GUS944 but contains only the first 192 amino acids of AHA2. This clone does not contain any of the 3′ untranslated sequences present in the full-length constructs; however, the 3′ region does not appear to have any significant effect on translation or transcription levels based on controls using an AHA2-promoter/GUS fusion.

Transgenic Plants

Transgenic plants were generated by a root transformation protocol (Valvekens et al., 1988) using liquid-grown roots and *Agrobacterium tumefaciens* LBA4404. Transgenic plants were regenerated on growth media containing kanamycin (50 $\mu g\ mL^{-1}$) and carbenicillin (500 $\mu g\ mL^{-1}$). Results presented here were obtained from transgenic plant lines 298 (AHA2-GUS944), 475-B1 and 475-D4 (AHA3-GUS904), 465-7305 (AHA3-c-*myc*904), and 205 (AHA2-GUS193). Additional lines mentioned in confirmatory experiments included 471–100 (AHA3-c-*myc*944) and 482 (AHA3-GUS944).

Protein Assays

All protein concentrations were determined by Lowry assays (Lowry et al., 1951) using 0.1% (w/v) sodium deoxycholate to solubilize membranes. BSA was used as a standard.

Microsomal Membrane Preparations

Microsomal membranes were prepared with modifications to a previously described procedure (Serrano, 1984). All manipulations were conducted on ice or in a cold room, with prechilled buffers. For Suc gradients, nonfrozen tissues were ground in a mortar and pestle. For western blot analysis, tissues were frozen in liquid nitrogen and pulverized in a coffee grinder with dry ice. Pulverized tissues were mixed with an equal weight of extraction buffer (290 mM Suc, 25 mM EDTA, 250 mM Tris-HCl, pH 8.5, 2 mM PMSF, and 76 mM β-mercaptoethanol). Tissues were further processed by grinding in a Tissumizer (Tekmar, Cincinnati, OH), in a mortar and pestle, or in a Dounce homogenizer. Homogenates were filtered through cheesecloth or nylon filters to remove large debris and then centrifuged at 5,000*g* to remove intact organelles and cell walls. Supernatants were spun at greater than 40,000*g* for at least 40 min to pellet microsomal membranes, which were then resuspended in homogenization buffer.

Membrane Fractionation

Plasma membranes were separated from other membranes by Suc gradients or aqueous two-phase partitioning (Schaller and DeWitt, 1995). Normally, gradients were loaded with membranes extracted from 20 g fresh weight of tissue. Aqueous two-phase partitioning was conducted with 5 to 10 g fresh weight of tissue per preparation with yields of approximately 75 μg of membrane proteins in the upper phase. For gradients, microsomes were applied to a 17-mL linear Suc gradient containing either 15 to 45% (w/w) or 20 to 45% (w/w) Suc, in centrifugation buffer (1 mM DTT, 1 mM EDTA, and 10 mM Tris-HCl, pH 7.5). Suc gradients were centrifuged in a swinging bucket rotor at 150,000*g* for 5 h. Fractions of 1 to 1.2 mL were collected and either assayed immediately or frozen at −70°C.

Western and Slot Blots

SDS-PAGE samples were mixed with 3× loading buffer (100 mM Tris, pH 6.8, 3.7% [w/v] SDS, 5% [w/v] DTT, 20% [w/v] Suc or glycerol, 0.3% [w/v] bromphenol blue) and incubated for 15 min at 25°C. After electrophoresis (Laemmli 1970), proteins were transferred to PVDF membranes (Immobilon-P, Millipore) or nitrocellulose (Schleicher & Schuell) using a minigel transfer apparatus (Hoefer or Bio-Rad). Transfer buffer consisted of 192 mM Gly, 25 mM Tris-HCl, pH 8.3, 20% (v/v) methanol, and 0.02% (w/v) SDS. Slot blots were made with a slot-blot apparatus (Bio-Rad). Membrane pellets were resuspended in 10 mM Tris-HCl, pH 7.0, 1 mM EGTA, 1 mM EDTA, and 20% (w/w) glycerol, diluted at least 10-fold with 3 M guanidine HCl, 50 mM Tris-HCl, pH 7.0, and suctioned through a nitrocellulose sheet in the blotting apparatus.

Immunodetection

Western and slot blots were blocked for at least 12 h in TBS-T (20 mM Tris, pH 7.6, 137 mM NaCl, 0.1% (w/v) Tween 20) with 5% (w/v) nonfat dry milk. Primary antisera were normally diluted in blocking buffer at the following concentrations: anti-CTF2, at 1:5000; anti-GUS, at 1:2000; and anti-c-*myc* 9E10.2, at 1:2000. Secondary antibodies were used at a dilution of 1:2000 in blocking buffer. For AHA3 blots using the c-*myc* 9E10.2 antibody, after the primary step, an intermediate antiserum incubation step was included: rabbit anti-mouse IgG, 1:2000; 1-h incubation, followed by four 15-min washes in TBS-T. Primary and secondary antibody incubations were for 1 h at room temperature and were followed by four 15-min washes in TBS-T. Secondary antibodies were detected using enhanced chemiluminescence (ECL, Amersham) or alkaline phosphatase reagents (Promega). Some blots were reprobed after incubation at 50°C for 30 min in stripping buffer (100 mM 2-mercaptoethanol, 2% (w/v) SDS, 62.5 mM Tris-HCl, pH 6.7), followed by two 15-min washes in large volumes of TBS-T at room temperature.

Marker Enzyme Assays

Standard assays are described in detail elsewhere (Schaller and DeWitt, 1995) and are only briefly described below.

GUS activity was fluorometrically assayed at 37°C in 0.55-mL volume reactions containing 50 mM sodium phosphate, pH 7.0, 10 mM β-mercaptoethanol, 10 mM Na_2EDTA, 0.1% (w/v) sodium lauryl sarcosine, 0.1% (w/v) Triton X-100 (Sigma), and the substrate 1 mM 4-methylumbelliferyl glucuronide (Jefferson, 1987). Activity was reported as moles of 4-methylumbelliferone produced. In controls, assays were conducted with the addition of 1% Triton X-100 to confirm that membrane vesicles were disrupted and that latent GUS activity was measured. Fluorescence was measured on a DNA fluorometer model TKO100 (Hoefer Scientific, San Francisco, CA). As a control for background levels of activity, fractions from wild-type plants were assayed in parallel.

NADH Cyt *c* reductase activity was assayed at room temperature in 1-mL reaction volumes, containing 20 mM KPO_4, pH 7.2, 0.2 mM NADH, 0.02 mM Cyt *c*, 10 mM KCN, and 1 mM antimycin A (Lord et al., 1973). Each fraction (100 μL) was added to start the reaction. Activity was recorded as $\Delta(A_{550}-A_{600})$ using a spectrophotometer (model 552, Perkin Elmer) operating in dual-beam mode.

Chlorophyll *a* and *b* concentrations were determined spectrophotometrically with 10-μL samples mixed with 750 μL of 95% ethanol, and the A_{645} and A_{663} were measured. Chlorophyll *a* and *b* content was determined using the equation $C_{a+b} = 5.24A_{664.2} + 22.24A_{648.6}$, with concentrations given as μg/mL plant extract solution (Lichtenthaler, 1987).

Fusicoccin-binding assays were conducted as described previously (Feyerabend and Weiler, 1988). ^{3}H-labeled fusicoccin was kindly provided by Prof. R. Cleland (University of Washington, Seattle). Samples of each fraction (100 μL) were added to 0.9 mL of binding buffer containing 10 mM Tris-Mes, pH 6, 1 mM $CaCl_2$, 1 mM $MgSO_4$, 1 mM EDTA, 1 mM KF, 2.6 mM DTT, and 10 nM [^{3}H]fusicoccin (35.2 Ci/mM). Tubes were incubated for 1 h on ice and then centrifuged in a microfuge for 1 h. The bottom of the tubes containing drained pellets were cut off and sonicated in scintillation fluid (Ecoscint, National Diagnostics, Atlanta, GA). Radioactivity was determined using a scintillation counter (model LS1801, Beckman). Fusicoccin binding to membranes was calculated as the amount of [^{3}H]fusicoccin binding that was competed off the membranes with 10 mM nonradioactive fusicoccin.

Triton-stimulated UDPase activity was assayed using 1- to 10-μL samples of membrane fractions added to 100 μL of assay buffer consisting of 3 mM UDP, 3 mM $MnSO_4$, 30 mM Mes-Tris, pH 6.5 (Nagahashi and Kane, 1982). A parallel reaction was conducted with the addition of 0.03% (w/v) Triton X-100. Reactions were incubated at 37°C for 20 min and released phosphate was determined using the malachite green method (Lanzetta et al., 1979). Triton-stimulated UDPase activity was calculated as the difference in activity between the presence and absence of detergent.

H^+-ATPase assays for Suc gradients were carried out with 1- to 5-μL samples of membrane fractions added to 0.5 mL of 5 mM ATP, 5 mM $MgCl_2$, 10 mM Pipes, pH 7.5, 5 mM NaN_3, 0.1 sodium molybdate. Vanadate-sensitive ATPase activity was determined by the addition of 100 μM Na_3VO_4. Assays were performed at 30°C for 30 min and released phosphate was detected using a molybdate/semidine reaction (Dryer et al., 1957).

RESULTS

Immunolocalization of an H^+-ATPase Subfamily

In our first approach to investigating the localization of P-type H^+-ATPases, we generated a polyclonal antiserum, termed anti-CTF2, that was directed against the highly divergent C-terminal domain of isoform AHA2. In the following experiments we show that anti-CTF2 reacts specifically with a subfamily of P-type H^+-ATPases, which, as a group, co-localize to the plasma membrane.

Anti-CTF2 was used to probe a western blot of total protein extracted from roots, leaves, siliques, and flowers, as shown in Figure 1. A single band of approximately 100 kD was detected in all tissues, consistent with the predicted size for all P-type H^+-ATPases cloned from plants.

Although the anti-CTF-2 serum was directed against an AHA2 antigen, it appears to cross-react with AHA3. In the western blots shown in Figure 2, the anti-CTF2 serum cross-reacts with a 170-kD band corresponding to a GUS-tagged AHA3 fusion (AHA3-GUS904) expressed in transgenic plants. As a control, the 170-kD band was also shown to cross-react with antiserum raised against the large central cytoplasmic loop of isoform AHA3 (anti-CLF3, for central loop fusion of AHA3, provided by R. Serrano as antibody 721). All chimeric AHA3 proteins were expressed at similar levels in transgenic plants, estimated to be less than 5% that of the total endogenous ATPase detected by anti-CTF-3 at the 100-kD position.

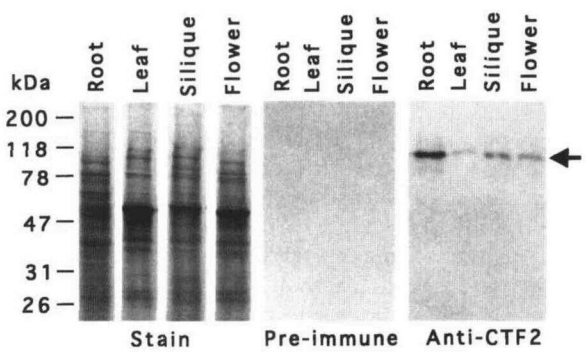

Figure 1. Western blot of total cellular protein showing specificity of the anti-CTF2 antiserum. Total cellular protein was obtained by homogenization with a mortar and pestle in 300 mM Suc, 10 mM EDTA, 2 mM EGTA, 100 mM Tris, pH 7.8, 1 mM PMSF, and 35 mM β-mercaptoethanol. The extract was clarified by a low-speed centrifugation to pellet cell-wall debris. Samples (20 μg each) were electrophoresed in a 10% (w/w) polyacrylamide-SDS gel. One gel was stained with Coomassie blue, and a parallel gel was transferred to nitrocellulose and probed with anti-CTF2. The western blot was developed with enhanced chemiluminescence. The arrow points to immunoreacting ATPases at 100 kD.

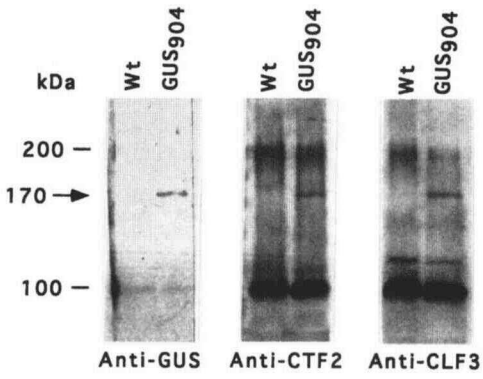

Figure 2. Western blot of AHA3-GUS904 microsomal membranes demonstrating that AHA3 is detected by anti-CTF2 antiserum. Samples (15 μg) of microsomal membranes were electrophoresed in a 6% (w/w) polyacrylamide-SDS gel and transferred to PVDF membranes. Three blots were probed in parallel with anti-GUS antiserum, anti-CTF2, and anti-CLF3. The arrow points to the position of a 170-kD band detected by all three antisera in extracts from AHA3-GUS904 plants (GUS_{904} lane) but not from control wild-type plants (Wt). The major band seen at 100 kD corresponds to plasma membrane H^+-ATPases. A diffuse band at 200 kD and above is commonly observed and is thought to be ATPase aggregates.

Western blot analysis was also used to show that anti-CTF2 cross-reacts with AHA1 (data not shown). In this case an AHA1 cDNA was expressed in Sf-9 insect cells (*Spodoptera fugiperda*), using a baculovirus expression system (Invitragen). On western blots of total extractable protein, AHA1 was detected by anti-CTF2 as a single 100-kD band.

Although anti-CTF2 clearly cross-reacts with AHA1, AHA-2, and AHA-3, it does not detect at least one isoform, AHA10. As shown by western blot analysis, anti-CTF2 failed to recognize a fusion protein containing the AHA10 C-terminal domain (data not shown). This result is not surprising since AHA10 is the most divergent pump identified in the AHA family, with only 42% identity to AHA2 in the C-terminal domain (Harper et al., 1994).

Evidence from aqueous two-phase partitioning indicates that as a group the P-type H^+-ATPases detected by anti-CTF2 reside in the plasma membrane. Figure 3 shows a western blot of upper- and lower-phase fractions probed with anti-CTF2. A single immunoreactive band of 100 kD showed a significant enrichment in the upper-phase fraction, which with this fractionation technique is diagnostic of plasma membrane association. Control experiments were performed to confirm that our fractionation procedure faithfully partitioned a conventional plasma membrane marker (molybdate-insensitive, vanadate-sensitive ATPase activity) to the upper phase and two nonplasma membrane markers to the lower phase (a representative control is shown in Fig. 8). However, our results do not exclude the possibility that this subfamily of pumps is localized on an uncharacterized endomembrane vesicle that co-partitions with the plasma membrane into the upper phase.

Figure 4 shows immunocytological evidence that members of the anti-CTF2 immunoreactive subfamily of P-type H^+-ATPases are preferentially localized to the plasma membrane. Tissue sections were fixed with a paraformaldehyde-based protocol that was chosen as a compromise between obtaining good cell structure and preserving antigenicity for the anti-CTF2 antiserum. Since some tissue preparations contained plasmolyzed cells, it was possible to verify that labeling occurred in the region of the plasma membrane and not the cell wall. The labeling analysis of 43 companion cells, surveyed from two independent experiments using plasmolyzed cells, is summarized in Table I. Gold particles were found preferentially associated with the plasma membrane region 5 times more frequently than with either the cell wall or internal cellular locations. Companion cells were analyzed because of the strong labeling observed for this cell type. Previously, immunofluorescence microscopy of leaf and stem sections indicated that this subfamily of pumps is most abundant in cell types engaged in significant transport processes (e.g. companion cells and guard cells) (DeWitt and Sussman, 1995).

Localization of Epitope-Tagged AHA2

Although we demonstrated that the plasma membrane is the predominant location for a subfamily of P-type H^+-ATPases that cross-reacts with anti-CTF2, our first approach did not provide information about the localization of specific isoforms such as AHA2. Therefore, we next examined the targeting of individual isoforms by engineering them with immunological tags and expressing them in transgenic plants. In the next two sections we present results indicating that the tagged versions of isoforms AHA2 and AHA3 are preferentially localized to the plasma membrane.

Figure 5 shows a restriction map of the DNA construct pAHA2-GUS944, which encodes a GUS-tagged AHA2 under the control of its natural 5′ and 3′ regulatory sequences. For all studies of AHA2-GUS944 membranes were purified

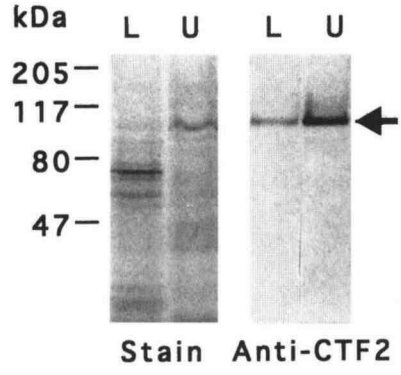

Figure 3. Western blot of membranes fractionated by aqueous two-phase partitioning showing plasma membrane localization of the anti-CTF2 detectable subfamily of P-type ATPases. Samples (20 μg each) of lower-phase (L) and upper-phase (U) fractions were electrophoresed in a 10% (w/w) polyacrylamide-SDS gel. One gel was stained with Coomassie blue to show the enrichment of a 100-kD band in the upper phase. A gel run in parallel was transferred to nitrocellulose, probed with anti-CTF2, and developed with an alkaline phosphatase system (Promega). The arrow marks the immunoreactive 100-kD band, which shows a dramatic enrichment in the upper phase.

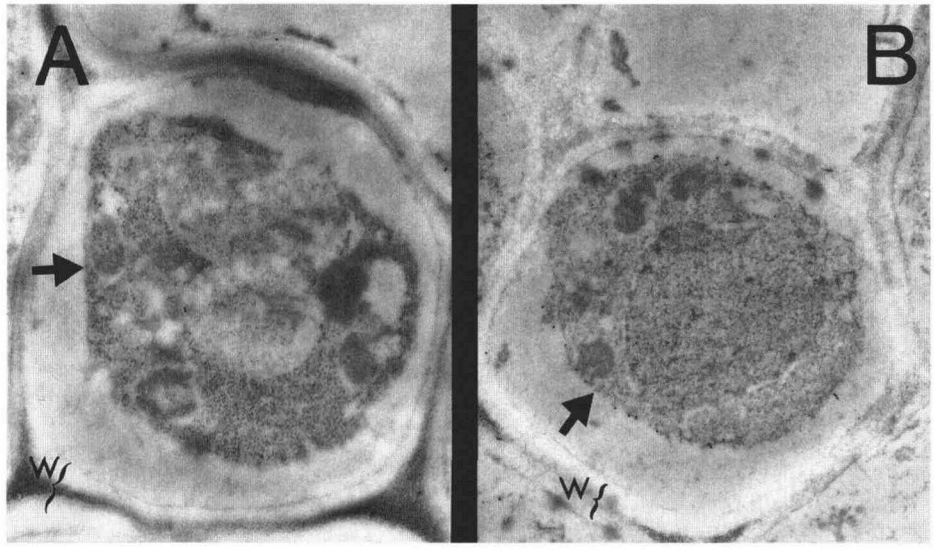

Figure 4. Immunogold localization of P-type H^+-ATPases in plasmolyzed companion cells. A, A control section from an Arabidopsis stem labeled with preimmune serum and gold-conjugated secondary antibody. The arrow points to the plasma membrane region that has retracted from the cell wall. Note the absence of label in the plasma membrane region. B, A section processed in parallel to the control but labeled with anti-CTF2 and gold-conjugated secondary antibody. Note the gold particles on the plasma membrane (arrow points to plasma membrane region) and the absence of gold particles on the cell wall (marked "w") and cytoplasm.

from transgenic plant material grown in sterile liquid cultures, in which approximately 90% of the biomass is derived from the root. Consistent with northern blot analysis for the endogenous AHA2 (Harper et al., 1990), AHA2-GUS944 protein was expressed at high levels in roots. However, unlike the endogenous AHA2, AHA2-GUS944 was expressed ectopically throughout the plant (J.F. Harper, unpublished data). Therefore, our results are based on the expression of AHA2-GUS944 in both "native" and "nonnative" cell types.

Figure 6 shows that AHA2-GUS944 expressed in transgenic plants can be specifically detected by anti-GUS antibodies on a western blot of microsomal membrane proteins. Membranes containing AHA2-GUS944 showed a strong signal at the expected molecular mass of 170 kD, whereas control wild-type membranes showed no signal at this molecular mass. In Figure 6, the control lane was stained longer than the transgenic lane to demonstrate that the weaker background bands were clearly at positions different from the 170-kD AHA2-GUS944 band.

To determine whether AHA2-GUS944 was targeted to the plasma membrane, we fractionated membranes by an aqueous two-phase partitioning procedure. Figure 7 shows representative slot blots of membrane fractions from plants expressing AHA2-GUS944 and from wild-type control plants. The four fractions analyzed were soluble proteins, microsomal membranes, upper phase, and lower phase. Samples were blotted in a dilution series and probed with anti-GUS or anti-CTF2 antiserum.

Our slot-blot analysis showed that AHA2-GUS944 was 10- to 50-fold enriched in the upper phase (plasma membrane) compared with the lower phase, as detected by an anti-GUS probe. This level of enrichment is equivalent to that seen in a parallel slot blot of wild-type membranes probed with anti-CTF2 and is therefore consistent with AHA2-GUS944 being associated with the plasma membrane.

The following control experiments were done to verify the efficacy of our immunodetection and two-phase partitioning procedures. First, the specificity of the anti-GUS antiserum was verified by probing slot blots from a parallel fractionation of wild-type membranes (Fig. 7). Nonspecific signals from wild-type membrane fractions were less than 2% that of the corresponding fractions containing AHA2-GUS944. Second, control assays indicate that our two-phase system faithfully partitioned a standard plasma membrane marker into the upper phase and markers for the Golgi apparatus and the ER into the lower phase (Fig. 8A).

Additional control experiments, shown in Figure 8, were conducted to determine whether quantitation of AHA2-GUS944 levels by immunodetection would agree with those from GUS activity assays. Surprisingly, we observed a discrepancy between these two methods. The largest discrepancy (20-fold) was observed between measurements of relative GUS levels in the microsomal membrane

Table I. *Quantification of anti-CTF2 immunogold labeling of companion cells*

Serum	No. of Cells	Plasma Membrane		Internal		Cell Wall	
		Total	Average	Total	Average	Total	Average
Preimmune	6	6	1	4	0.7	7	1.2
Anti-CTF2	43	683	16	110	2.6	61	1.4

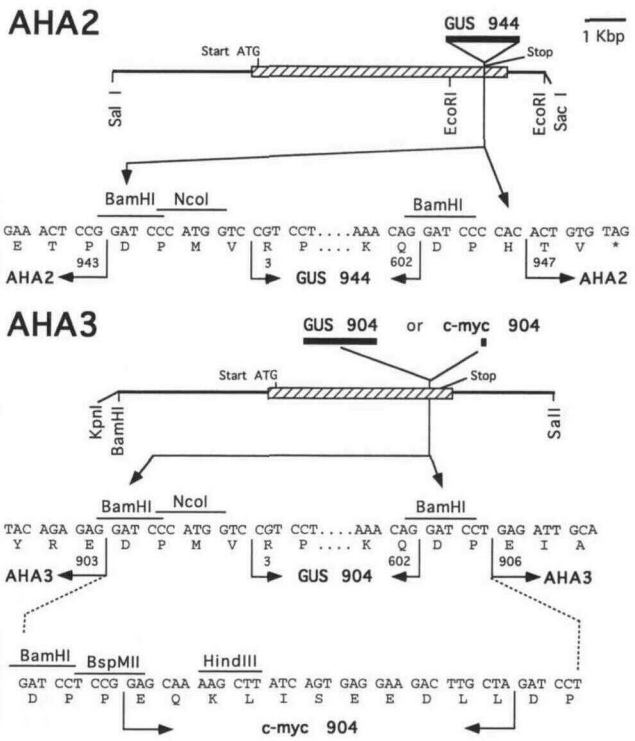

Figure 5. Diagram of epitope-tagged AHA2 and AHA3 constructs. The GUS-tagged AHA2 is shown on top (pAHA2-GUS944), and GUS- and c-*myc*-tagged AHA3s are shown below (pAHA3-GUS904 and pAHA3-c-*myc*904). The cross-hatched boxes represent the transcribed regions, including introns. The "944" and "904" designations indicate the amino acid sequence position where the tags are inserted. Each gene is expressed under the control of its natural upstream promoter elements.

and soluble fractions (Fig. 9C). Whereas a 50-fold enrichment of GUS in the membrane fraction was observed for the GUS epitope, only a 2.4-fold enrichment was observed for GUS activity. A 5-fold discrepancy was observed between different methods of quantifying GUS in the upper- and lower-phase fractions (Fig. 9B). Nevertheless, activity measurements still showed an enrichment of AHA2-GUS944 in the upper phase and therefore support its plasma membrane localization.

Localization of Epitope-Tagged AHA3s

Studies of AHA3 gave results equivalent to those of AHA2 and also enabled us to compare the performance of multiple immunological tags engineered into two different locations. Figure 5 shows a restriction map of DNA constructs encoding AHA3-GUS904 and AHA3-c-*myc*904. Additional constructs giving similar results are described elsewhere (i.e. GUS and c-*myc* at the 944 position and the influenza hemagglutinin virus epitope at 904 and 944 locations; DeWitt, 1994)

For studies of tagged AHA3s microsomal membranes were purified from leaf and stem tissues obtained from transgenic plants grown in soil. As shown by immunofluorescence and histochemical staining (DeWitt and Sussman, 1995) the c-*myc*- and GUS-tagged AHA3 constructs retain the phloem-specific expression predicted by reporter gene studies (DeWitt et al., 1991). Thus, the targeting properties of our tagged AHA3s were analyzed in their "native" cell type.

GUS- and c-*myc*-tagged AHA3s were specifically identified as either 170- or 100-kD bands by their respective antiserum (Fig. 3; DeWitt and Sussman, 1995). Detection of the c-*myc*-tagged pumps was quite clear. In contrast, two different anti-GUS antibodies showed a significant amount of nonspecific background, which precluded the use of slot blots to quantify the GUS-tagged AHA3s. This background was insignificant for our slot-blot analysis of AHA2-GUS944 since the AHA2 construct was expressed at a greater than 10-fold higher level than GUS-tagged AHA3s.

To test whether epitope-tagged AHA3s were targeted to the plasma membrane we fractionated microsomal membranes by equilibrium buoyant density centrifugation. Figure 9 shows representative results from three fractionation experiments, all of which show co-fractionation of tagged AHA3s with plasma membrane markers.

In gradient A (Fig. 9A) AHA3-GUS904 was detected by measuring GUS enzyme activity; the peak activity was observed between 34 and 36% Suc. This peak overlaps with the position of plasma membrane H$^+$-ATPases, as shown by a western blot probed with anti-CTF2. This gradient profile shows that the overlapping GUS activity and plasma membrane peaks were clearly separated from markers corresponding to the ER (NADH Cyt *c* reductase) at 28% Suc and chloroplast membranes (chlorophyll *a* plus *b*) at 43% Suc. On separate gradients it was confirmed that

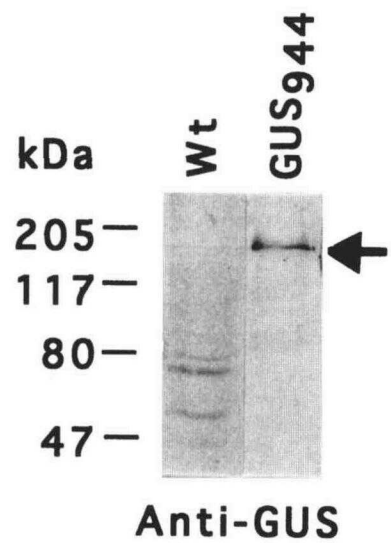

Figure 6. Western blot of microsomal membranes showing the specific detection of AHA2-GUS944 by anti-GUS antiserum. Samples (20 μg each) of microsomal membranes from wild-type (Wt) or AHA2-GUS944 plant line 298 (GUS_{944}) were electrophoresed in a 10% (w/w) polyacrylamide-SDS gel, transferred to nitrocellulose, and probed with anti-GUS antiserum. Blots were developed with an alkaline phosphatase system (Promega). The wild-type lane was developed longer to show the position of weaker background bands. The arrow marks the immunoreactive 170-kD band corresponding to AHA2-GUS944.

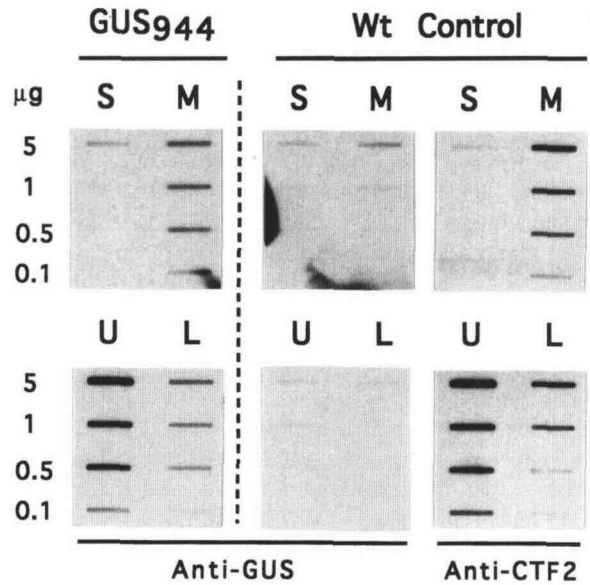

Figure 7. Slot-blot quantitation of GUS-tagged AHA2 in membranes fractionated by aqueous two-phase partitioning. The columns marked on top by GUS_{944} show slot-blotted protein obtained from fractionation of transgenic plants expressing AHA2-GUS944 (plant line 298). The four columns marked on top by Wt show slot-blotted protein obtained from control fractionations of wild-type plants. Fractionations of AHA2-GUS944 and wild-type plants were run in parallel. Individual columns are marked to indicate the protein fraction: soluble (S), microsomal membrane (M), upper (U), and lower (L). A dilution series from 5 to 0.1 µg of protein from each fraction was transferred to nitrocellulose using a slot-blot apparatus (Bio-Rad). The columns marked on the bottom as "Anti-GUS" were probed with anti-GUS antiserum. Note the weak background signal in all of the wild-type control fractions. The columns marked on the bottom as "Anti-CTF2" were probed with anti-CTF2 antiserum. These blots provide a control to show that the fractionation protocol partitioned a plasma membrane marker into the upper (U) phase. The slot blots shown were developed using enhanced chemiluminescence.

the GUS activity was cleanly separated from a tonoplast marker (nitrate-inhibited ATPase) at 20 to 24% Suc (not shown). As shown in gradient B, our gradient system also cleanly separated plasma membrane markers from a Golgi marker (Triton-stimulated UDPase) at 25 to 28% Suc.

In gradient B (Fig. 9B) AHA3-c-*myc*904 was detected by western blots probed for the c-*myc* epitope. The peak abundance of AHA3-c-*myc*904 was between 33 and 38% Suc. This peak overlaps with (a) the peak position of the fusicoccin-binding protein (a plasma membrane marker, at 33% Suc) and (b) a broad peak for the endogenous plasma membrane H^+-ATPase marker detected by the anti-CTF2 antiserum. Although the AHA3-c-*myc*904 is also recognized by the anti-CTF2 antibody, we estimate that the tagged isoform contributes less than 5% of the total anti-CTF2 signal and therefore should not bias the distribution pattern observed with the general H^+-ATPase probe. Thus, AHA3-c-*myc*904 appears to co-fractionate with two independent plasma membrane markers.

In gradient C (Fig. (C) the relative locations of AHA3-GUS904 and AHA3-c-*myc*904 were directly compared by separating both markers on the same gradient. Both the GUS activity and c-*myc* epitope peaks equilibrated to coincident positions between 34 and 38% Suc, although on some gradients the exact peak of the c-*myc* appeared slightly heavier than the GUS peak. The fusicoccin-binding protein was assayed as a second marker for the plasma membrane and confirmed that both c-*myc* and GUS-tagged pumps co-migrate with plasma membranes in our gradient fractionation system.

In addition to the analysis of all four tagged AHA3s by Suc gradient fractionation, AHA3-GUS904 was further characterized by aqueous two-phase partitioning (data not shown). The GUS enzyme activity showed a 2-fold enrichment in the upper phase. Although this level of enrichment fell short of the 10- to 50-fold enrichment seen for control markers (e.g. vanadate-sensitive ATPase and anti-CTF2 im-

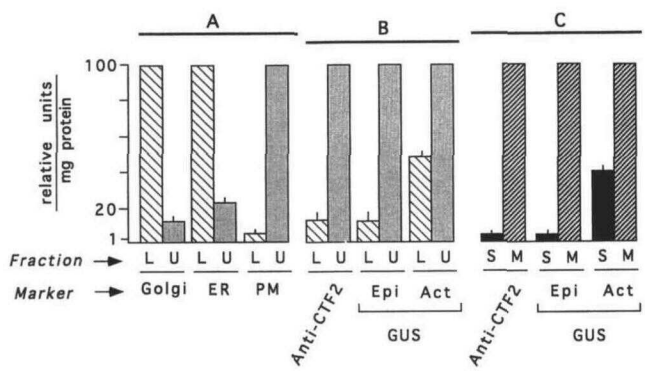

Figure 8. Controls for aqueous two-phase partitioning. Fractions analyzed are indicated at the bottom: lower phase (L), upper phase (U), soluble (S), and microsomal membrane (M). This graph is plotted in relative units to show the degree of partitioning between fractions (i.e. lower versus upper phase and soluble versus membrane). A, A representative control to show that the fractionation protocol partitioned the Golgi apparatus and ER into the lower phase and a plasma membrane marker into the upper phase. The marker for the Golgi apparatus was Triton-stimulated UDPase, which showed 1.1 (± 0.1) mmol min^{-1} mg^{-1} in the lower fraction. The marker for ER was NADH Cyt *c* reductase, which showed 0.16 (±.04) mmol min^{-1} mg^{-1} in the lower fraction. The marker for the plasma membrane was vanadate-sensitive ATPase, which showed 1.6 (± 0.2) µmol min^{-1} mg^{-1} in the upper phase. B and C, A representative control showing a discrepancy between two methods of measuring relative levels of a GUS-tagged ATPase. For comparison the fractions probed with anti-CTF2 are from wild-type plants processed in parallel with an AHA2-GUS944 plant. This comparison provides a control to show the relative enrichment expected for a plasma membrane protein. Relative levels of immunodetectable pump were determined from slot blots shown in Figure 7. These relative values are in close agreement with those determined by assays for vanadate-sensitive ATPase activity. The remaining fractions in B and C are from a fractionation of AHA2-GUS944 plant material. These fractions were probed for the GUS marker by two methods; those probed by immunodetection of GUS epitope are marked "Epi," and those assayed for GUS activity are marked "Act". The level of GUS activity observed in the upper phase (U) and microsomal membrane fractions (M) were 56 (± 6) and 19 (± 2) nmol min^{-1} mg^{-1}, respectively. Note that the relative levels of AHA2-GUS944 determined by immunodetection of GUS epitope most closely match those determined for plasma membrane markers.

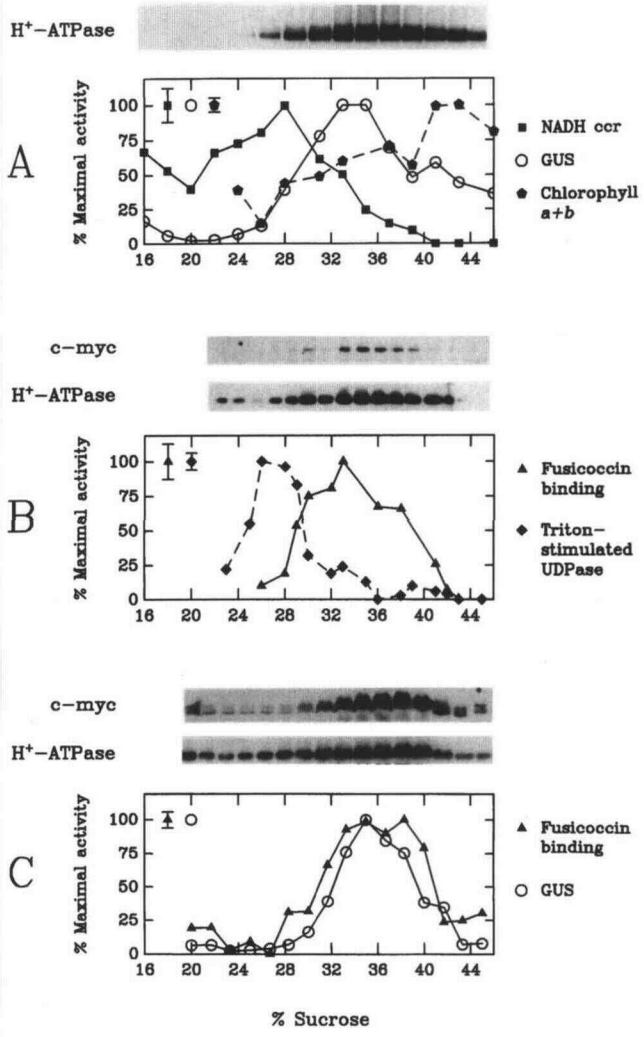

Figure 9. Suc gradient fractionation of AHA3-c-*myc*904 and AHA3-GUS904 showing co-fractionation with plasma membrane markers. Representative error bars for each assay are indicated in the upper left of each plot. Western blots showing the 100-kD position are aligned on top of the plots. Samples of 70 or 210 μL from each 1-mL fraction were electrophoresed in a 10% (w/w) polyacrylamide-SDS gel and transferred to nitrocellulose. Blots marked "H$^+$-ATPase" were probed with anti-CTF2 antiserum, and those marked "c-*myc*" were probed with the anti-c-*myc* monoclonal antibody. A, Microsomal membranes from plants expressing AHA3-GUS904 were fractionated over a 15 to 45% (w/w) Suc gradient. GUS enzyme activity assays yielded 1.42 pmol min^{-1} mL^{-1} in the peak fractions (33–35% Suc). Spectrophotometric measurement of chlorophyll *a* and *b* yielded 272 μg/mL at the peak fraction (43% Suc). NADH-Cyt *c* reductase (NADH ccr) activity yielded 0.25 μmol min^{-1} mL^{-1} at the peak fraction (at 28% Suc). B, Crude membrane preparations from plants expressing AHA3-c-*myc*904 were fractionated over a 20 to 45% (w/w) Suc gradient. Maximal competible fusicoccin binding (at 34% Suc) was 1.3 pmol/mL. Maximal Triton-stimulated UDPase activity (at 26% Suc) was 0.41 μmol min^{-1} mL^{-1} fraction. C, Crude membrane preparations from plants expressing AHA3-c-*myc*904 and AHA3-GUS904 were mixed and fractionated over the same 20 to 45% (w/w) Suc gradient. GUS enzyme activity assays yielded 0.43 pmol min^{-1} mL^{-1} fraction in the peak fraction (35% Suc). Maximal competible fusicoccin binding was 1.8 pmol mL^{-1} in the peak fractions (35–38% Suc).

munoreactive protein), it is in close agreement with the level of enrichment observed for AHA2-GUS944 when determined by GUS activity assays.

Localization of a Truncated AHA2

It is not known whether targeting of integral membrane proteins to the plasma membrane is mediated in plants by specific sorting or retention information or if it occurs by a default pathway (Chrispeels et al., 1995). As a first step toward understanding how P-type H$^+$-ATPases are localized to the plasma membrane, we compared the targeting of a full-length AHA2-GUS944 with that of the truncated AHA2-GUS193, which contained only the first two predicted transmembrane domains of AHA2 (residues 1–193) fused to GUS.

Microsomal membranes were purified from transgenic plants grown in sterile liquid culture, which expressed the AHA2-GUS193. Aqueous two-phase partitioning and buoyant density centrifugation of these membranes showed that, although this truncated ATPase was associated with microsomal membranes, it failed to localize to the plasma membrane (Fig. 10). GUS activity was more than 100-fold higher in the lower phase compared with the upper phase, indicating that the truncated fusion is not associated with the plasma membrane. In controls, the upper phase showed a typical 10- to 50-fold enrichment for H$^+$-ATPases, as determined by slot blots probed with the anti-CTF2 antiserum. Western blot analysis confirmed that AHA2-GUS193 was most abundant in the lower phase (data not shown). Quantification by slot-blot analysis was

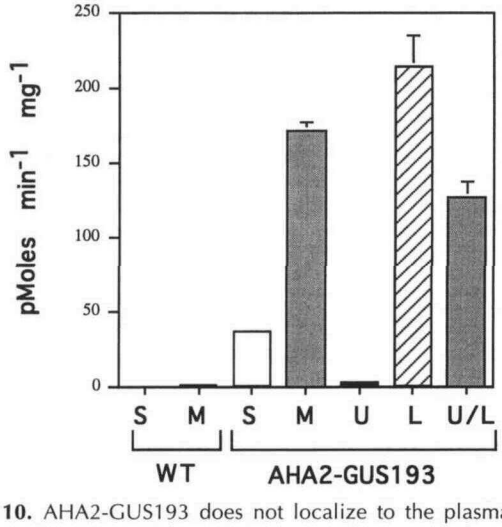

Figure 10. AHA2-GUS193 does not localize to the plasma membrane as shown by GUS activity in membranes fractionated by aqueous two-phase partitioning. GUS activity was measured in extracts from wild-type (WT) and AHA2-GUS193 plants. Fractions are indicated by soluble (S), microsomal membranes (M), upper phase (U), and lower phase (L). "U/L" is a control in which an equal ratio of protein from the upper and lower phases were mixed prior to assays. This mixing control indicates that the upper phase was not contaminated by an inhibitor or protease, since the resulting activity of the mixed fractions showed the expected average of the two fractions assayed separately.

not possible because AHA2-GUS193 protein did not accumulate to high enough levels.

Suc gradients were used to independently verify the results of the aqueous two-phase partitioning (data not shown). The peak of GUS activity migrated to a Suc density of 20 to 24%. This density was clearly distinct from plasma membrane H^+-ATPase markers, which migrated to positions between 30 and 40%. Control experiments performed on fractions from the same gradient indicated that the GUS activity was found in a broad peak that overlapped with markers for the vacuole and ER, as determined by immunodetection on slot blots using antisera against α-tip (α-tonoplast intrinsic protein) and immunoglobulin heavy chain-binding protein, respectively (provided by M. Chrispeels).

In contrast to a full-length AHA2-GUS944, the truncated AHA2-GUS193 fusion protein appeared to be less stable. Although equivalent mRNA levels were expressed by both constructs in the plant lines analyzed (data not shown), the levels of GUS activity and immunodetectable fusion protein were reduced more than 50-fold for AHA2-GUS193.

DISCUSSION

AHA2 and AHA3 Localize to the Plasma Membrane

The primary objective of this research was to determine whether the H^+-ATPase isoforms AHA2 and AHA3 are localized to the plasma membrane. Although there was biochemical and genetic evidence to support their designation as H^+-ATPases, there has, to our knowledge, been no direct experimental evidence to verify their plasma membrane localization. In fact, when expressed in yeast these isoforms appeared to accumulate in an ER-like membrane instead of in the plasma membrane (Villalba et al., 1992).

Here we provide three lines of evidence indicating that AHA2 and AHA3 are both localized to the plasma membrane: (a) A major subfamily of P-type H^+-ATPases, defined by their cross-reaction with anti-CTF2 antiserum (and shown to include isoforms AHA2 and AHA3), co-fractionates with the plasma membrane in aqueous two-phase partitioning and buoyant density Suc gradients; (b) this subfamily of P-type H^+-ATPases was also shown to localize to the plasma membrane region by immunogold labeling and electron microscopy of sectioned companion cells; (c) epitope-tagged versions of AHA2 and AHA3 co-fractionate with plasma membranes, as shown by aqueous two-phase partitioning and Suc gradients, respectively.

Epitope Tagging

Our second objective was to determine the best way to tag all of the H^+-ATPase isoforms by identifying a tag and a tagging location that would not alter the natural targeting properties of the pumps. To address this concern we compared the targeting of four different versions of AHA3, which were independently tagged at two different locations with c-*myc* and GUS. All four tagged versions appeared to be targeted to the plasma membrane, as indicated by Suc gradients. This co-fractionation with the plasma membrane was confirmed by aqueous two-phase partitioning for one of the GUS-tagged AHA3s. Plasma membrane localization of the c-*myc*-tagged AHA3 isoform was further verified by immunofluorescent microscopic studies, in which the c-*myc* antiserum was observed to strongly label the cell periphery (DeWitt and Sussman, 1995). But although all of our results are consistent with plasma membrane localization of AHA2 and AHA3 isoforms, we cannot rule out that the tagged isoforms were localized to an uncharacterized membrane system. For example, it is possible that tagged pumps could reside in secretory vesicles near the cell perimeter that co-fractionate with the plasma membrane. Nevertheless, within the limits of our methodologies, all of the AHA2 and AHA3 C-terminally tagged pumps appear to localize to the plasma membrane. Therefore, the C-terminal end of the plant P-type H^+-ATPases appears to be a suitable location for the addition of small (e.g. c-*myc*) and large (e.g. GUS) immunologically detectable tags.

Although both c-*myc* and GUS worked well as epitope tags, the c-*myc* tag is recommended because (a) its small size and lack of dimerization potential make it is less likely to disrupt protein structure; (b) it gave the most specific and sensitive detection on western blot analysis; and (c) it was cleanly detected by indirect immunofluorescence (DeWitt and Sussman, 1995). (We were unable to detect either c-*myc* or GUS tagged AHA3s by immunogold-labeling and electron microscopy.)

Although the GUS tag can function as both an epitope and an enzymatic marker, our results suggest that the specific activity of the GUS domain may be reduced when it is tethered to a H^+-ATPase. In estimating the relative levels of AHA2-GUS944, we observed as much as a 20-fold difference between levels of GUS-tagged pump based on immunodetection and GUS activity. The apparent lower activity of GUS when tethered to the pump may be due to a steric constraint that prevents the GUS domain from oligomerizing. Because of the observed discrepancy in GUS activity, we believe that immunodetection of GUS is the most reliable method of quantifying GUS-tagged proteins.

Targeting Information

Our third objective was to answer the question of how a plant P-type H^+-ATPase is localized to the plasma membrane. Our results favor a model in which specific information is required to localize a pump to the plasma membrane rather than a model in which the pump is targeted by a default pathway (Pfeffer and Rothman, 1987). To pursue this question, we examined the targeting properties of a truncated ATPase containing the first two transmembrane domains of AHA2 fused to GUS (AHA2-GUS193). When this truncated ATPase was expressed in transgenic plants, it was found to be associated with the microsomal membrane fraction. This indicates that AHA2-GUS193 can be inserted into membranes, which is consistent with a report that the first two transmembrane domains of the *Neurospora* H^+-ATPase can function as an isolated pair to promote membrane insertion (Lin and Addison, 1995). However, our results also show that the truncated pump fails to accumulate in the plant plasma membrane, suggesting that

additional information is required for its delivery or retention. This result is not surprising given the recent reports of several different mutations in the yeast plasma membrane H^+-ATPase that result in biosynthetic arrest, suggesting that the targeting of pumps is a sensitive process that undergoes quality control while in transit through the endomembrane system (Chang et al., 1993; Harris et al., 1994; Chang and Fink, 1995).

We speculate that AHA2-GUS193 is targeted by default to the tonoplast where it is degraded. This hypothesis is consistent with targeting studies in yeast, indicating that the tonoplast is a default destination for membrane proteins lacking specific information (Stack and Emr, 1993; Nothwehr and Stevens, 1994). Whether the tonoplast is the default location for membrane proteins in plants is still unknown (Höfte and Chrispeels, 1992; Chrispeels et al., 1995).

ACKNOWLEDGMENTS

We thank Jane Lloyd, Hong-Qing Guo, and Huyen Nguyen for technical assistance with membrane fractionations and GUS assays; Brad Binder and Donna Fernandez for help with producing the anti-CTF2 antisera; Maarten Chrispeels for providing α-tonoplast intrinsic protein and immunoglobulin heavy chain-binding protein antibodies; Ramon Serrano for providing antibody no. 721; and Fernando Camilo for preparing graphs.

Received January 22, 1996; accepted June 27, 1996.

LITERATURE CITED

Bevan M (1984) Binary *Agrobacterium* vectors for plant transformation. Nucleic Acids Res **12:** 8711–8720

Boutry M, Michelet B, Goffeau A (1989) Molecular cloning of a family of plant genes encoding a protein homologous to plasma membrane H^+-translocating ATPases. Biochem Biophys Res Commun **162:** 567–574

Briskin DP (1990) The plasma membrane H^+-ATPase of higher plant cells: biochemistry and transport function. Biochim Biophys Acta **1019:** 95–190

Chang A, Fink GR (1995) Targeting of the yeast plasma membrane [H^+]ATPase: a novel gene ASTI prevents mislocalization of mutant ATPase to the vacuole. J Cell Biol **128:** 39–49

Chang A, Rose MD, Slayman CW (1993) Folding and intracellular transport of the yeast plasma-membrane H^+-ATPase: effects of mutations in *KAR2* and *SEC65*. Proc Natl Acad Sci USA **90:** 5808–5812

Chrispeels MJ, Coruzzi G, Nasrallah J (1995) Plant cell biology comes of age. Plant Cell **7:** 237–248

DeWitt ND (1994) Epitope tagging and reporter gene studies identify an *Arabidopsis* plasma membrane proton pump specific for phloem companion cells. PhD thesis. University of Wisconsin, Madison

DeWitt ND, Harper JF, Sussman MR (1991) Evidence for a plasma membrane proton pump in phloem cells of higher plants. Plant J **1:** 121–128

DeWitt ND, Sussman MR (1995) Immuno-cytochemical localization of an epitope-tagged plasma membrane proton pump (H^+-ATPase) in phloem companion cells. Plant Cell **7:** 2053–2067

Dryer RL, Tammes AR, Routh JI (1957) The determination of phosphorus and phosphatase with *N*-phenyl-*p*-phenylenediamine. J Biol Chem **225:** 177–183

Ewing NN, Bennett AB (1994) Assessment of the number and expression of P-type H^+-ATPase genes in tomato. Plant Physiol **106:** 547–557

Feyerabend M, Weiler EW (1988) Characterization and localization of fusicoccin-binding sites in leaf tissues of *Vicia faba* L. probed with a novel radioligand. Planta **174:** 115–122

Hager A, Debus G, Edel H-G, Stransky H, Serrano R (1991) Auxin induces exocytosis and the rapid synthesis of a high turnover pool of plasma-membrane H^+-ATPase. Planta **185:** 527–537

Harper JF, Manney L, DeWitt ND, Yoo MH, Sussman MR (1990) The *Arabidopsis thaliana* plasma membrane H(+)-ATPase multigene family. Genomic sequence and expression of a third isoform. J Biol Chem **265:** 13601–13608

Harper JF, Manney L, Sussman MR (1994) The plasma membrane H^+-ATPase gene family in *Arabidopsis*: genomic sequence of *AHA 10* which is expressed primarily in developing seeds. Mol Gen Genet **244:** 572–587

Harper JF, Surowy TK, Sussman MR (1989) Molecular cloning and sequence of cDNA encoding the plasma membrane proton pump (H^+-ATPase) of *Arabidopsis thaliana*. Proc Natl Acad Sci USA **86:** 1234–1238

Harris SL, Na S, Zhu X, Steo-Young D, Perlin DS, Tem JH, Haber JE (1994) Dominant lethal mutations in the plasma membrane H^+-ATPase gene of *Saccharomyces cerevisiae*. Proc Natl Acad Sci USA **91:** 10531–10535

Höfte H, Chrispeels MJ (1992) Protein sorting to the vacuolar membrane. Plant Cell **4:** 995–1004

Holné G, Boutry M (1994) Identification of an *Arabidopsis thaliana* gene encoding a plasma membrane H^+-ATPase whose expression is restricted to anther tissue. Plant J **5:** 311–317

Jefferson RA (1987) Assaying chimeric genes in plants: the GUS gene fusion system. Plant Mol Biol Rep **5:** 397–405

Kolodziej P, Young RA (1991) Epitope tagging and protein surveillance. Methods Enzymol **194:** 508–519

Kunkel TA, Roberts JD, Zakour RA (1987) Rapid and efficient site-specific mutagenesis without phenotypic selection. Methods Enzymol **154:** 367–382

Laemmli UK (1970) Cleavage of structural proteins during the assembly of the head of bacteriophage T4. Nature **227:** 680–685

Lanzetta PA, Alvarez LJ, Reinach PS, Candia OA (1979) An improved assay for nanomole amounts of inorganic phosphate. Anal Biochem **100:** 95–97

Lichtenthaler HK (1987) Chlorophylls and carotenoids: pigments of photosynthetic biomembranes. *In* L Packer, R Douce, eds, Methods in Enzymology, Academic Press, San Diego, CA, pp 350–382

Lin J, Addison R (1995) A novel integration signal that is composed of two transmembrane segments is required to integrate the *Neurospora* plasma membrane H^+-ATPase into microsomes. J Biol Chem **270:** 6935–6941

Lord JM, Kagawa T, Moore TS, Beevers H (1973) Endoplasmic reticulum as the site of lecithin formation in castor bean endosperm. J Cell Biol **57:** 659–667

Lowry OH, Rosebrough NJ, Farr A, Randall RJ (1951) Protein measurement with the Folin phenol reagent. J Biol Chem **193:** 265–275

Michelet B, Boutry M (1995) The plasma membrane H^+-ATPase. A highly regulated enzyme with multiple physiology functions. Plant Physiol **108:** 1–6

Nagahashi J, Kane AP (1982) Triton-stimulated nucleoside diphosphatase activity: subcellular localization in corn root homogenates. Protoplasma **112:** 167–173

Nothwehr SF, Stevens TH (1994) Sorting of membrane proteins in the yeast secretory pathway. J Biol Chem **269:** 10185–10188

Palmgren MG, Christensen G (1993) Complementation in situ of the yeast plasma membrane H^+-ATPase gene *pma1* by a H^+-ATPase gene from a heterologous species. FEBS Lett **317:** 216–222

Palmgren MG, Christensen G (1994) Functional comparisons between plant plasma membrane H^+-ATPase isoforms expressed in yeast. J Biol Chem **269:** 3027–3033

Pardo JM, Serrano R (1989) Structure of a plasma membrane H^+-ATPase gene from the plant *Arabidopsis thaliana*. J Biol Chem **264:** 8557–8562

Pfeffer S, Rothman JE (1987) Biosynthetic protein transport and sorting by the endoplasmic reticulum and Golgi. Annu Rev Biochem **56:** 829–852

Sambrook J, Fritsch EF, Maniatis T (1989) Molecular Cloning: A Laboratory Manual. Cold Spring Harbor Laboratory, Cold Spring Harbor, NY

Schaller GE, DeWitt ND (1995) Analysis of the H^+-ATPase and other proteins of the *Arabidopsis* plasma membrane. Methods Cell Biol **50:** 129–148

Serrano R (1984) Purification of the proton pumping ATPase from plant plasma membranes. Biochem Biophys Res Commun **121:** 735–740

Smith DB, Johnson KS (1988) Single-step purification of polypeptides expressed in *Escherichia coli* as fusions with glutathione transferase. Gene **67:** 31–40

Stack JH, Emr SD (1993) Genetic and biochemical studies of protein sorting to the yeast vacuole. Curr Opin Cell Biol **5:** 641–664

Sussman MR, DeWitt ND, Harper JF (1994) Calcium protons and potassium as inorganic second messengers in the cytoplasm of plant cells. *In* EM Myerowitz, CR Somerville, eds, Arabidopsis, Cold Spring Harbor Laboratory Press, Cold Spring Harbor, NY, pp 1085–1117

Valvekens D, Van Montagu M, Van Ligsebettens M (1988) *Agrobacterium tumefaciens*-mediated transformation of *Arabidopsis thaliana* root explants by using kanamycin selection. Proc Natl Acad Sci USA **85:** 5536–5540

Villalba JM, Palmgren MG, Berberian GE, Fergusen C, Serrano R (1992) Functional expression of plant plasma membrane H^+-ATPase in yeast endoplasmatic reticulum. J Biol Chem **267:** 12341–12349

Wada M, Shono M, Urayama O, Satoh S, Hara Y, Ikawa Y, Fujii T (1994) Molecular cloning of P-type ATPases on intracellular membranes of the marine alga *Heterosigma akashiwo*. Plant Mol Biol **26:** 699–708